Cell Transplantation, Vol. 19, pp. 549–564, 2010
Printed in the USA.

0963-6897/10 $90.00 + .00
DOI: 10.3727/096368910X491383
E-ISSN 1555-3892
www.cognizantcommunication.com

Transplant of GABAergic Precursors Restores Hippocampal Inhibitory Function in a Mouse Model of Seizure Susceptibility

I. Zipancic,*†[1] M. E. Calcagnotto,*[1] M. Piquer-Gil,* L. E. Mello,‡ and M. Álvarez-Dolado*

*Department of Cell Therapy and Regenerative Medicine, Andalusian Center for Molecular Biology and Regenerative Medicine (CABIMER), Seville, Spain
†Centro de Investigación Príncipe Felipe (CIPF), Valencia, Spain
‡Department of Physiology, Universidade Federal de São Paulo (UNIFESP), São Paulo, Brazil

Defects in GABAergic function can cause epilepsy. In the last years, cell-based therapies have attempted to correct these defects with disparate success on animal models of epilepsy. Recently, we demonstrated that medial ganglionic eminence (MGE)-derived cells grafted into the neonatal normal brain migrate and differentiate into functional mature GABAergic interneurons. These cells are able to modulate the local level of GABA-mediated synaptic inhibition, which suggests their suitability for cell-based therapies. However, it is unclear whether they can integrate in the host circuitry and rescue the loss of inhibition in pathological conditions. Thus, as proof of principle, we grafted MGE-derived cells into a mouse model of seizure susceptibility caused by specific elimination of GABAergic interneuron subpopulations in the mouse hippocampus after injection of the neurotoxic saporin conjugated to substance P (SSP-Sap). This ablation was associated with significant decrease in inhibitory postsynaptic currents (IPSC) on CA1 pyramidal cells and increased seizure susceptibility induced by pentylenetetrazol (PTZ). Grafting of GFP^+ MGE-derived cells in SSP-Sap-treated mice repopulates the hippocampal ablated zone with cells expressing molecular markers of mature interneurons. Interestingly, IPSC kinetics on CA1 pyramidal cells of ablated hippocampus significantly increased after transplantation, reaching levels similar to the normal mice. More importantly, this was associated with reduction in seizure severity and decrease in postseizure mortality induced by PTZ. Our data show that MGE-derived cells fulfill most of the requirements for an appropriate cell-based therapy, and indicate their suitability for neurological conditions where a modulation of synaptic inhibition is needed, such as epilepsy.

Key words: Cell therapy; GABA; Epilepsy; Interneuron; Medial ganglionic eminence (MGE); Saporin

INTRODUCTION

The GABAergic system plays an important role in the etiology of epilepsy. Numerous studies have shown altered number and function of GABAergic interneurons in the cortex and hippocampus of animal models and patients with epilepsy (4,5,11,12,15,20,25,53). These defects lead to an imbalance between inhibitory and excitatory circuits that may cause epilepsy (31,39).

Among the therapeutic approaches for epilepsy treatment, antiepileptic drugs (AED) that target the GABAergic system present an acceptable efficacy. However, despite the progresses in AED application, up to a third of patients continue to experience seizures on maximal tolerated drug therapy (23). Refractory epilepsy remains a large clinical problem, because surgical resection is only appropriate for a minority of patients (14,35). Therefore, novel therapeutic approaches are urgently needed for a substantial number of epileptic patients (19).

In recent years, cell-based therapies have been investigated as a way to modulate hyperactivity or increase the inhibitory activity as a potential antiepileptic approach (22,38,40,45). Cell grafts from different sources have been performed with disparate effects in animal models of epilepsy (22,38,40,45). Embryonic stem (ES) cells, fetal hippocampal precursors, or cells genetically modified to produce and secrete GABA have been transplanted into the hippocampus or in regions implicated in the generalization of seizures (10,16,18,24,27,41,43,

Received August 27, 2009; final acceptance February 5, 2010. Online prepub date: February 8, 2010.
[1]These authors provided equal contribution.
Address correspondence to Manuel Álvarez-Dolado, Centro de Biología Molecular y Medicina Regenerativa (CABIMER), Av. Americo Vespucio s/n-41092 Seville, Spain. Tel: +34 954-467829; E-mail: manuel.alvarez@cabimer.es

45–47,52). These cell types were partially successful in reverting some of the pathological changes observed in the animal models. However, they presented important drawbacks, such as their poor tissue distribution or, in the case of ES cells, the lack of safety due to potential generation of teratocarcinomas (8,41). In addition, the grafts have only a transient effect, maybe due to decreased GABA release over time, or because the host target neurons downregulate their own GABA receptors following transplantation (21,27). Finally, the functionality and interaction of these grafted cells with the host circuitry never was described in detail at the electrophysiological level.

These limitations make necessary the search for alternative sources of cells with antiepileptic potential. Good candidates to overcome these difficulties, and achieve higher levels of inhibition or modulate the excitatory activity, are the GABAergic interneurons. In the last few years, it has been shown that most of the GABAergic interneurons in the cortex and hippocampus are derived from neuronal precursors born in the medial ganglionic eminence (MGE) (3,9,28,51). We recently demonstrated that MGE-derived precursors can be transplanted into the neonatal normal brain, giving rise to neurons that can migrate and differentiate into fully mature GABAergic interneurons throughout the cortical plate and the hippocampus (2). More importantly, these cells are able to integrate into the local circuits and make functional synapses with existing neurons, influencing the level of GABA-mediated synaptic inhibition (2). In addition, they have been recently transplanted in an animal model of stroke, with partial success in the amelioration of the neurological symptoms (13). These observations strongly suggest the suitability of these precursors for their use in cell-based antiepileptic therapies. However, whether MGE-derived interneurons are able to differentiate properly, integrate in the circuitry satisfactorily, and modify the inhibitory synaptic function under neuropathological conditions remains unknown.

To address this issue, we performed grafts of MGE-derived precursors into a new mouse model of hippocampal disinhibition, associated with hyperexcitability and susceptibility to seizures induced by pentylenetetrazol (PTZ). This mouse model, based on the rat model developed by Martin and Sloviter (29), was generated by a selective and spatially located ablation of hippocampal neurons expressing substance P receptors, a subpopulation of GABAergic inhibitory interneurons (1,34, 44). Although the model does not completely resemble all the characteristics of epilepsy, we consider it appropriate for evaluating the MGE-derived precursor capacity to recover the loss of inhibition, and to verify their ability to replace the specific loss of GABAergic interneurons. After transplantation in this mouse model, we examined the survival, distribution, morphology, and molecular phenotype of the graft-derived cells at different time points. In addition, we evaluated their possible effects on the inhibitory synaptic function and seizure susceptibility of the mice. This information will be critical to verify the suitability of MGE-derived precursors for cell replacement therapies and their potential contribution to the functional recovery of epileptic brain.

MATERIALS AND METHODS

Animals and Experimental Groups

CD-1 adult mice (60 days old) were obtained from Charles River (Barcelona, Spain) and kept in the CIPF animal facility. All animal procedures were carried out in accordance with the Spanish legislation (RD 1201/05 and L 32/07) and the guidelines of CIPF animal care committee.

We established three experimental groups. The first group (SSP-Sap + MGE) comprised mice with specific interneuron ablation by a substance P analogue, SSP [Sar^9, $Met(O_2)^{11}$], conjugated to the neurotoxin saporin, a type I ribosome-inactivating protein (SSP-Sap; Advanced Targeting Systems, Inc.). This group ($n = 17$), 7 days later, received a transplant of MGE-derived cells. The second group (SSP-Sap, $n = 11$) constituted by mice with SSP-Sap-mediated ablation received, 7 days later, a similar volume of dead cells (by repeated frost and thaw cycles) as a control of inflammatory response or GFP toxicity. Finally, the third group (Control, $n = 10$) was comprised of sham-operated mice.

SSP-Sap Injection

We adapted the procedure developed by Martin and Sloviter in the rat (29). Basically, mice were anesthetized (1.5–2% isoflurane) and positioned under a stereotaxic apparatus (Stoelting). Skull was exposed and trepanned with the help of a Dremel. A total of 40–50 nl volume of SSP-Sap (0.04 mg/ml in sterile PBS) was injected with a sharpened glass micropipette (~20 μm diameter), prefilled with mineral oil. The micropipette was attached to a Narishige oil microinjector and coupled to the stereotaxic apparatus. We injected bilaterally in two different points, corresponding to the anterior and posterior hippocampus. The 40–50-nl volume was injected in four to five points of the dorsal axe at the following coordinates from bregma (L: +/–1.3; A: –2.06; D: –2.1/–1.8/–1.5/–1.2/–0.9, and L: +/–2.8; A: –2.8; D: –2.3/–2.0/–1.8/–1.5), according to the compact mouse brain atlas by Paxinos and Franklin (36).

Cell Isolation and Transplant

MGE-derived cells were isolated as previously described (2) from E12.5 embryonic GFP^+ transgenic mice (17). At this age, generation of GABAergic precursors

is at its maximum and a sulcus clearly separates MGE from LGE, facilitating a clean dissection. Cell number and viability (~80%) was checked by trypan blue exclusion before transplantation. Highly concentrated cell suspension (~10^5 cells/μl) was front-loaded into beveled glass micropipettes (~60 μm diameter) prefilled with mineral oil and L-15 medium. Then $4–8 \times 10^4$ cells per mouse were injected bilaterally in the same coordinates used for SSP-Sap injection. After surgical procedure, grafted mice were returned to their cages and analyzed 2, 4, and 12 months later.

Immunostaining

Perfusion, brain collection, sectioning, and immunostaining were performed as previously described (2). We used the following antibodies: rabbit anti-GABA (1:1000, Sigma), anti-neurokinin-1 (NK-1; 1:1000, Chemicon), anti-neuropeptide Y (NPY; 1:300, ImmunoStar), anti-somatostatin 28 (SOM; 1:2000, Chemicon), and anti-calretinin (CR; 1:200, Swant); and mouse anti-parvalbumin (PV; 1:4000, Sigma), anti-GFP (1:200, AbCam), anti-glial fibrillary acidic protein (GFAP; 1:500, Chemicon), and anti-Iba1 (1:200, Wako). The following secondary antibodies were used: cy3-conjugated donkey anti-mouse or anti-rabbit, and biotin-conjugated donkey anti-mouse (Jackson ImmunoResearch, PA). For DAB immunohistochemistry, incubation with ABC complex (Vector) was performed. For NK-1 detection, due its low expression level, an incubation with ABC complex and amplification of the signal by tyramide reaction was performed (TSA kit, Invitrogen).

Cell Counts and Quantifications

Quantifications of cell bodies positive for GFP and/or immunolabeled for interneuron markers were performed on digitized images obtained with a DFC480 digital camera and IM500/FW4000 image manager software (Leica Microsystems Imaging Solutions, Cambridge, UK) on a DM6000B microscope (Leica Microsystems, Wetzlar, Germany).

Survival percentage of grafted cells, at 2, 4, and 12 months after the transplant, was estimated in serial sections, as previously described (2). We counted all the GFP^+ cells in the anterior–posterior and septo–temporal axis of one of this series (seven coronal slices of 50 μm, two of them including the injection sites, separated each section 300 μm, and covering from −1.06 mm to −3.28 mm with respect to bregma in the longitudinal axe). A representation of cell number versus distance to injection site was obtained on graph paper. Quantification of area under the graph was estimated as total number of survived cells. The percentage of grafted GFP^+ cells expressing GABA, PV, CR, NK-1, SOM, or NPY was calculated in each mouse ($n = 4$) in three coronal sections, between the two injection sites (see above), in the whole CA1 and hilus regions of the hippocampus. At least 500 GFP^+ cells were analyzed per marker and animal.

Electrophysiology

Slice Preparation. Acute tissue slices were prepared from CD-1 mice 2 and 4 months after the ablation and with or without transplantation, as described previously (2,12). Briefly, the mice were decapitated under anesthesia, and the brain was rapidly removed in ice-cold oxygenated (95% O_2/5% CO_2) slicing artificial cerebrospinal fluid (sACSF) (2,12). Horizontal hippocampal (300-μm-thick) slices were cut in 4°C oxygenated sACSF. The slices were immediately transferred to a holding chamber where they remained submerged in oxygenated normal recording ACSF (nACSF) (2,12). Slices were held at 37°C for 45 min and then at room temperature.

Whole-Cell Recordings. Recordings were obtained from hippocampal CA1 pyramidal cells visually identified using an epifluorescence and infrared differential interference contrast (IR-DIC) video microscopy system (Nikon). Patch pipettes (3.7 MΩ) were pulled from borosilicate glass capillary tubing (World Precision Instruments) using a micropipette puller (P-97; Sutter Instruments, Novato, CA), fire polished, and filled with intracellular solution for whole-cell voltage-clamp IPSC recordings (2,12). To isolate GABAergic currents, slices were perfused with nACSF containing 20 μM 6,7-dinitroquinoxaline-2,3-dione (DNQX) and 50 μM D-(−)-2-amino-5-phosphonovaleric acid (D-APV), and spontaneous and miniature IPSC (sIPSC and mIPSC) were recorded at a holding potential of 0 mV (the reversal potential for glutamate-mediated currents). mIPSC were recorded in nACSF containing 1 μM tetrodotoxin (TTX). At the majority of experiments 10 μM bicuculline methiodide (BMI) was applied to abolish IPSC, to confirm the involvement of $GABA_A$ receptors. For control the IPSC were recorded on CA1 pyramidal neurons in either the contra lateral hippocampus or in "age-matched" untreated animal. Voltage and current were recorded with an Multiclamp 700B amplifier (Molecular Devices) and monitored with an oscilloscope and with pClamp 10.0 software (Molecular Devices), running on a Pentium personal computer (Dell Computer Company, Round Rock, TX). Whole-cell voltage-clamp data were low-pass filtered at 1 kHz (−3 dB, eight-pole Bessel), digitally sampled at 20 kHz. Whole-cell access resistance was carefully monitored throughout the recording, and cells were rejected if values changed by more than 25% (or exceeded 20 MΩ); only recordings with stable series resistance of <20 MΩ were used for analysis.

Whole-cell currents were analyzed using Mini Analysis 6.0.7 (Synaptosoft, Decatur, GA) (e.g., a software

program that detects and measures spontaneous events as described previously) (2,12). Between 100 and 200 individual events were analyzed for each cell. Results are presented as the mean ± SEM. To compare results between cells from different animals, we used a one-way ANOVA followed by Tukey-Kramer test, with significance level of $p < 0.05$.

PTZ-Induced Seizure Susceptibility Test

Pentylenetetrazol (PTZ, 60 mg/kg, IP) was injected in 24 male CD-1 adult mice (nine controls, nine SSP-Sap, and 6 SSP-Sap + MGE cells), as described elsewhere (30). Immediately after injection, the animals were individually placed in a cage and their behavior was observed and video-recorded for 1 h. These video recordings were subsequently used to confirm the visual evaluation of the seizure severity, expressed by the following scale: (0) no abnormal behavior; (1) automatisms; (2) myoclonic twitches (sudden muscle jerk, sometimes accompanied by tail movements and head nodding); (3) unilateral forelimb clonus/bilateral forelimb clonus; (4) bilateral forelimb clonus and rearing; (5) rearing, falling, and generalized convulsions that could result in death. Each animal received a final score that correspond to its most severe seizure presented during the test. For all the animals with scores of 1 or above, the latency to the first seizure, regardless of severity, was also measured (in seconds). To compare results between groups, we used Fisher's exact test with significance level of $p < 0.05$.

RESULTS

Generation of a Mouse Model of Decreased Inhibition and Seizure Susceptibility

In order to test the capacity of MGE-derived progenitors to recover deficiencies in inhibition and replace the specific loss of GABAergic interneurons, both defects implicated in some types of epilepsy (12,20,25), we generated a mouse model of decreased inhibition and high seizure susceptibility by interneuron-specific ablation. For this, we injected the neurotoxic conjugate SSP-Sap into the anterior and posterior hippocampus of CD-1 adult mice (P60) (see Materials and Methods). As previously reported in the rat, 1 week after SSP-Sap injection, we observed a complete loss of GABAergic interneurons expressing substance P receptor, NK-1, in wide areas of the hippocampus (Fig. 1A–D).

In order to confirm the specificity of the ablation, we performed immunohistochemistry against specific markers of GABAergic interneurons. The loss of NK1-postive interneurons and the presence or absence of other interneuron subpopulations was the primary criteria used to establish the efficacy and selectivity of SSP-Sap-mediated ablation. Similar to previous results in rats (29), we observed a complete depletion of NPY- , SOM- , and NK-1$^+$ interneurons (Fig. 1A–H) around the SSP-Sap injection sites, and no alteration in the number of CR$^+$ cells (Fig. 2A, B). In contrast, opposite to what Martin and Sloviter (29 reported in the rat, we only observed a slight diminution in the number of PV$^+$ interneurons (Fig. 2C–D). This was due to the lack of NK-1 coexpression in most of the PV$^+$ interneurons. Only 16.1 ± 1.0% ($n = 4$) of these cells colocalized for NK-1 in the mouse hippocampus (Fig. 2E–G).

The area of ablation covered regions such as CA1, CA3, hilus, and dentate gyrus. A schematic representation of the extension of the interneuronal elimination is illustrated in Fig. 3 (shadowed area). The depletion of cells and the micropipette used to inject SSP-Sap produced no gross morphological anomalies in the hippocampus, confirmed by Nissl staining and the absence of reactive gliosis (data not shown).

In the rat, the specific ablation of hippocampal interneuron subpopulations by SSP-Sap leads to disinhibition and hyperexcitability in response to afferent stimulation (29). In addition, decrease in the number of interneurons use to be associated with a reduction of GABA-mediated synaptic inhibition (5,11,12). In order to confirm a similar alteration of the inhibitory activity in our mouse model, we performed patch clamp recordings of the pyramidal neurons in the CA1 area of the hippocampus. To ensure that electrophysiological recordings were effectively located in the region of interneuron ablation, we fixed and cut the slices after the recordings to perform inmunohistochemistry against NK-1, which confirmed the absence of this interneuron population in the area.

Whole-cell inhibitory postsynaptic currents (IPSC) on CA1 pyramidal cells from SSP-Sap-treated mice ($n = 5$) and sham-operated, age-matched controls ($n = 7$) were recorded 2 months after SSP-Sap injection (Fig. 4A). Analysis of sIPSC showed significant reductions in frequency and amplitude in CA1 pyramidal cells from SSP-Sap-treated mice. Average sIPSC frequency was reduced (1.78 ± 0.20 Hz; $n = 17$) when compared with controls (4.04 ± 0.36 Hz; $n = 20$; $p < 0.001$) (Fig. 4B), and average sIPSC amplitude was also significantly reduced in CA1 pyramidal cells from SSP-Sap-treated mice (10.06 ± 0.62 pA, $n = 17$) when compared with controls (16.23 ± 1.08 pA, $n = 20$; $p < 0.001$) (Fig. 4C). Finally, histograms of sIPSC amplitude showed a shift to small-amplitude events in SSP-Sap-treated mice (Fig. 4D).

To further characterize the reduction in GABA-mediated synaptic inhibition, TTX (1 μM) was added to the nACSF to isolate mIPSC. Significant decreases in mIPSC frequency were observed in CA1 pyramidal cells from SSP-Sap-treated mice (1.52 ± 0.15 Hz; $n = 17$) when

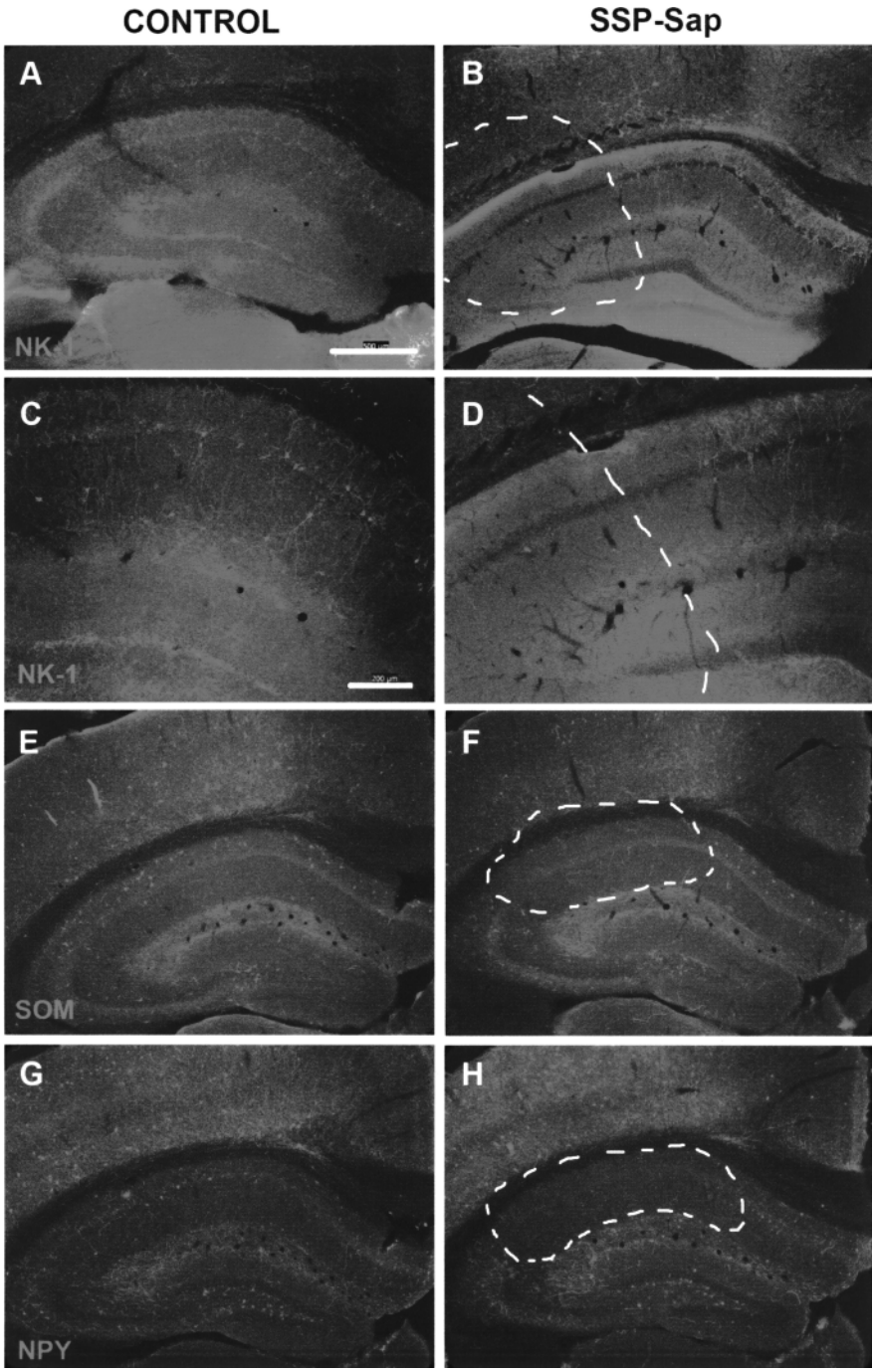

Figure 1. Specific interneuron ablation in the mouse hippocampus 7 days after SSP-Sap injection. (A–D) NK-1 immunofluorescence detection in hippocampal sections from control (A, C), and SSP-Sap-treated (B, D) mice, respectively. (C, D) High magnification photographs of (A) and (B), respectively. (E–H) SOM (E, F) and NPY (G, H) immunofluorescence detection in adjacent sections from control (E, G) and SSP-Sap-treated mouse (F, H), respectively. Note the elimination of immunopositive cells in the ablation area delimitated by the broken line. Scale bars: (A) 500 μm for (A, B, E, H); (C) 200 μm for (C, D).

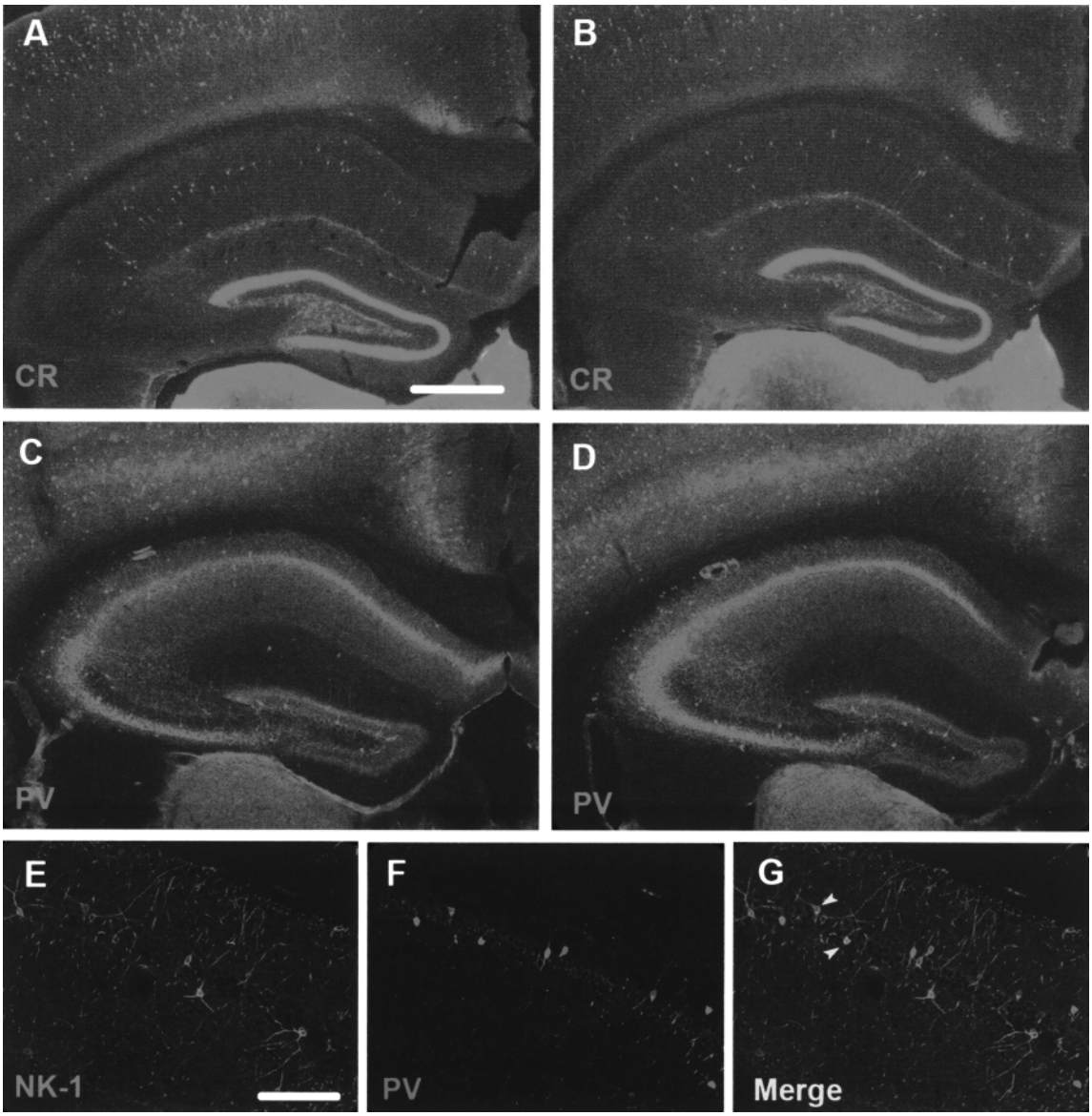

Figure 2. Survival of CR+ cells and partial ablation of PV^+ interneurons 7 days after SSP-Sap injection. (A, B) CR immunostaining of control (A) and SSP-Sap-injected hippocampus (B). (C, D) PV immunostaining of adjacent control (C) and SSP-Sap-treated hippocampus (D). Note the incomplete ablation of this subpopulation after SSP-Sap treatment. (E–G) Double immunohistochemical analysis for $NK\text{-}1^+$ (E) and PV^+ (F) interneurons in the CA1 region of the normal mouse hippocampus shows partial colocalization (arrowheads in G). Scale bars: (A) 500 μm for (A–D); (E) 50 μm for (E–G).

compared with controls (3.41 ± 0.30 Hz; $n = 17$; $p < 0.001$) (Fig. 4E). Changes in mIPSC amplitude were not detected (SSP-Sap: 9.73 ± 0.28 pA; $n = 17$; control: 10.78 ± 0.65 pA; $n = 17$) (Fig. 4F, G). Cumulative probability plots and Kolmogorov-Smirnov (K.S.) statistical analysis further confirmed reductions in IPSC frequency (sIPSC and mIPSC: K.S. test $p < 0.001$) and amplitude (sIPSC: K.S. test $p < 0.001$) (Fig. 4B, C, E). No changes in distribution, or average IPSC decay time constant and rise time 10–90%, were found (Fig. 5). Slower kinetics and lower amplitude of IPSC usually indicate activation of axo-dendritic synapses, while faster kinetics and higher amplitude of IPSC are associated with axo-somatic synapses (20,50). There were no reductions in number of slow-decay and rise time, small-amplitude mIPSC events, characteristic of dendrite-innervating interneurons.

These electrophysiological data showed an important reduction in the hippocampal inhibitory synaptic input of the mice after SSP-Sap injection, which was consistent with the histological observations of reduction in

the number of GABAergic interneurons in the same area.

Migration and Characterization of MGE-Derived Cell Grafts in the Mouse Model

MGE-derived cells are good candidates for cell therapy strategies, given their ability to migrate and differentiate into interneurons that functionally integrate when transplanted into the normal mouse brain (2). However, to ensure their therapeutic suitability, it is necessary to verify that: a) they behave similarly under pathological conditions and b) they are able to revert the symptoms associated with the pathology. Thus, we performed a series of MGE-derived grafts from GFP$^+$ embryos into the

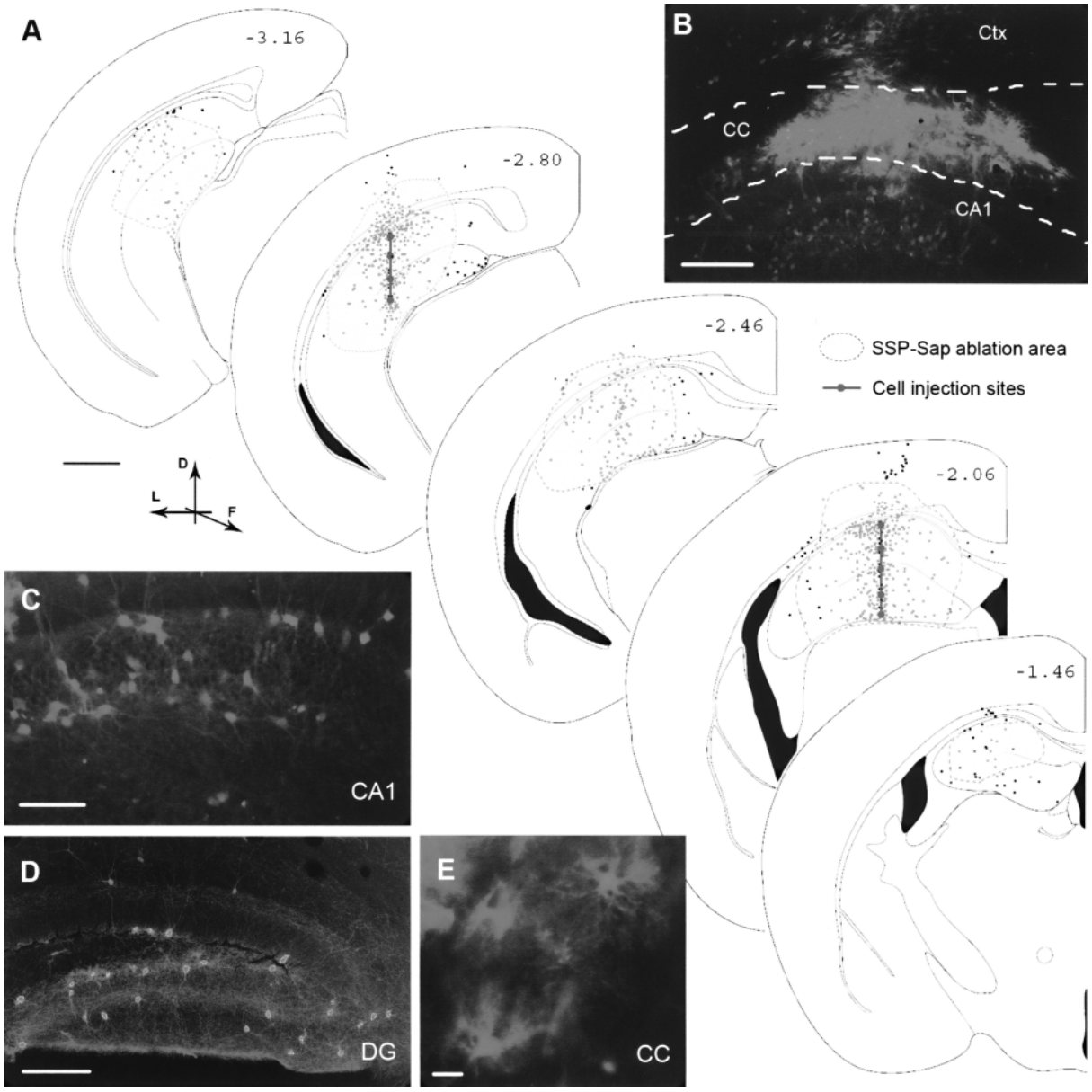

Figure 3. MGE-derived precursors repopulate the SSP-Sap-ablated hippocampus 60 days after the transplant. (A) Representative camera lucida maps showing the position of MGE graft-derived cells at five anterior–posterior levels through the hippocampus. The numbers in each slice indicate the stereological level respect to bregma in millimeters. Shadowed area corresponds to the SSP-Sap-ablated zone and verticle lines indicate the injection tracks, with the points of cell release represented by dots. MGE graft-derived cells spread out the injection site (B) and distribute randomly into the CA1 area (C), dentate gyrus (D), and corpus callosum (E). Note adult interneuron morphology of the grafted cells inside the hippocampus (C, D) and oligodendroglia-like morphology of the grafted cells in the corpus callosum (E). Scale bars: (A) 500 μm; (B) 100 μm; (C) 50 μm; (D) 75 μm, (E) 15 μm.

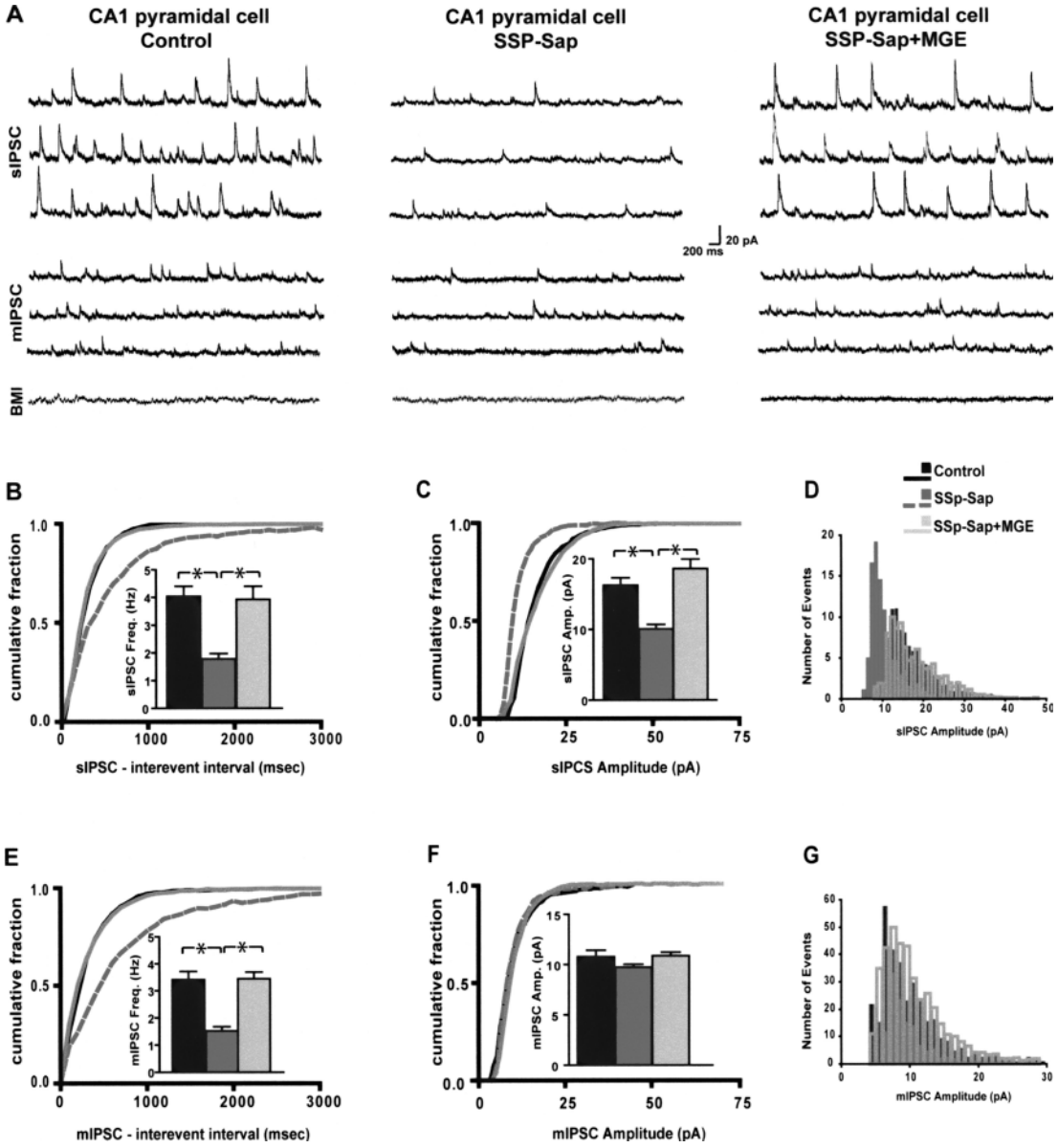

Figure 4. Synaptic inhibitory current is reduced after interneuron ablation in the hippocampus and it is restored 2 months after MGE-derived cell transplant. (A) Representative traces of sIPSC and mIPSC from CA1 pyramidal cells of control, SSP-Sap, and SSP-Sap + MGE experimental groups. (B, E) Cumulative fraction plots of sIPSC and mIPSC interevent intervals from CA1 pyramidal cells show lower frequency for SSP-Sap-treated mice, which reverted to normal values after MGE graft. Note that the curve of the frequency in SSP-Sap-treated mice is shifted to the right (lower frequency) and in SSP-Sap + MGE mice is shifted back to control values. Average sIPSC and mIPSC frequencies (insets) were also lower in CA1 pyramidal neurons from SSP-Sap-treated mice and increased after MGE grafts, as well. (C, F) Cumulative fraction plots of sIPSC and mIPSC amplitudes of from CA1 pyramidal cells show lower sIPSC amplitude for SSP-Sap-treated mice, which reverted to normal values after MGE graft. Note that the curve of the sIPSC amplitude in SSp-Sap-treated mice is shifted to the left (lower amplitude) and in SSP-Sap + MGE mice is shifted back to control values. Average sIPSC amplitude (inset) was also lower in CA1 pyramidal neurons from SSP-Sap-treated mice and increased after MGE grafts. No changes in mIPSC amplitude. (D, G) Distribution of sIPSC and mIPSC amplitudes from CA1 pyramidal cells. Control: black; SSP-Sap: dark gray; SSP-Sap + MGE: light gray. Error bars are SEM. $*p < 0.001$; one-way ANOVA followed by Tukey-Kramer test. BMI: bicuculline methiodide (10 μM).

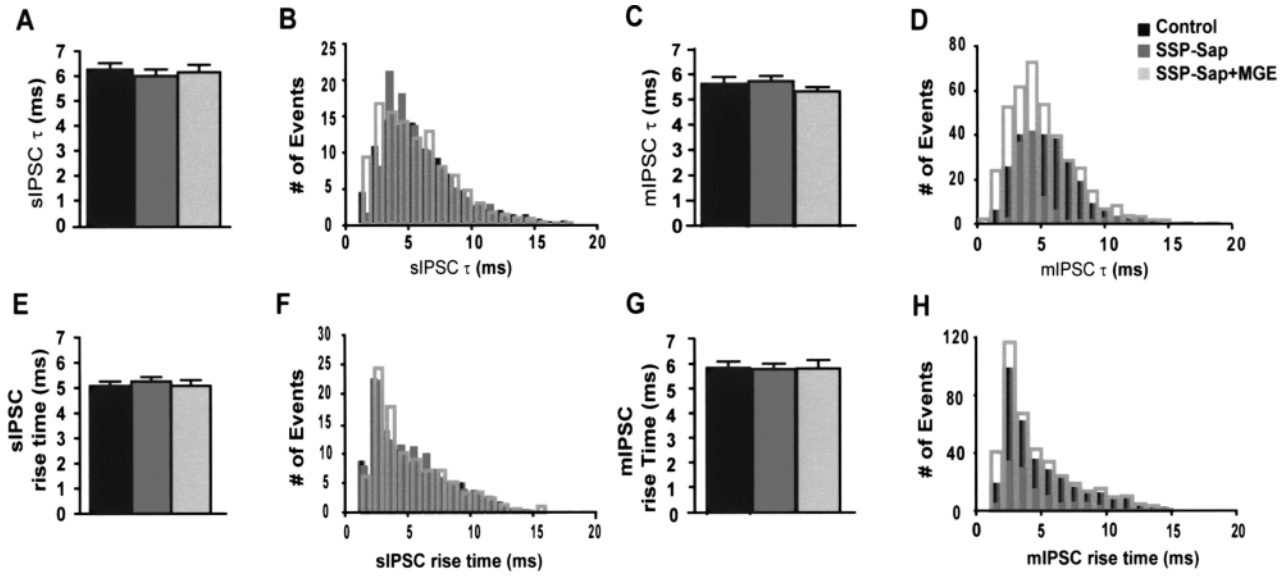

I - Decay time constant and rise time values of sIPSC and mIPSC in CA1 pyramidal cells

	Decay time constant (ms)			Rise time (10-90) (ms)		
	Control	SSP-Sap	SSP-Sap+MGE	Control	SSP-Sap	SSP-Sap+MGE
sIPSC	6.27 ± 0.26 (n=20)	6.02 ± 0.26 (n=17)	6.18 ± 0.30 (n=17)	5.07 ± 0.16 (n= 20)	5.26 ± 0.17 (n=17)	5.08 ± 0.24 (n=7)
mIPSC	5.72 ± 0.27 (n=13)	5.83 ± 0.21 (n= 17)	5.41 ± 0.17 (n=10)	5.94 ± 0.26 (n=17)	5.78 ± 0.23 (n=15)	5.81 ± 0.33 (n=14)

Figure 5. Average and distribution of decay time constant and rite time (10–90) of sIPSC and mIPSC in CA1 pyramidal cells of control, SSP-Sap-treated mice, and SSP-Sap + MGE groups 2 months after the transplant. (A–D) sIPSC and mIPSC decay time constant (*t*), and (E–H) rise time (10–90) for CA1 pyramidal cells have similar average and distribution in all three experimental groups: Control (black), SSP-Sap (dark gray), and SSP-Sap + MGE (light gray). Note the overplayed histograms (B, D, F, H). (I) Decay time constant and rise time values of sIPSC and mIPSC in CA1 pyramidal cells from age matched controls, and 2 months after SSP-Sap injection with no MGE grafts (SSP-Sap) and with MGE grafts (SSP-Sap + MGE). Similar values for all three groups (mean ± SEM). sIPSC, spontaneous IPSC; mIPCS, miniature IPSC; *n*, number of cells.

hippocampus of our mouse model of seizure susceptibility.

One week after SSP-Sap injection, we transplanted a total of $4–8 \times 10^4$ MGE-derived cells per brain into the anterior and posterior hippocampus, using the same stereotaxic coordinates for SSP-Sap injection. Analysis of grafted brains, 2 months after the transplant, revealed a widespread distribution of GFP^+ cells in the hippocampus, covering most of the ablation area (Fig. 3A). Survival rate of grafted cells was 20.3 ± 3.1% ($n = 5$) at this time point, evaluated in serial sections (see Materials and Methods) as the ratio of GFP^+ cells in the brain versus the number of transplanted cells. We also estimated the survival rate at 4 months (18.7 ± 2.6%, $n = 3$) and 1 year (18.1 ± 3.7%, $n = 3$) after the transplant with similar results. These data are comparable to others (2, 18,49) and indicate that grafted cells are stable and, very importantly, they suffer no transformation, given the fact that we never observed any tumor formation in the brain of the transplanted mice.

Similar to previous transplants in the normal neonatal brain (2), the GFP$^+$ cells presented a fully mature morphology 2 months after the transplant, showing large and elaborated dendritic trees that resemble the aspect of typical interneurons in the hippocampus (Fig. 3B–D). Approximately 86% of GFP$^+$ cells expressed the neuronal marker NeuN. In addition, we found endothelial cells around the injection site (CD31$^+$, 8%) and immature oligodendrocytes (Olig-2$^+$, 6%) within the corpus callosum (Fig. 3B, E), as previously reported (2). In contrast, none of the MGE-derived cells exhibited morphological or molecular features of pyramidal neurons or astrocytes (data not shown).

In order to confirm the acquisition of molecular properties of mature interneuron by the transplanted cells, we performed immunohistochemistry analysis. Double immunofluorescences revealed that 64.6 ± 4.7% of GFP$^+$ graft-derived cells expressed GABA (Fig. 6A). Subsets of the GFP$^+$ neurons also coexpressed PV (34.6 ± 5.6%), SOM (34.3 ± 6.2%), NPY (18.8 ± 2.9%), NK-1 (25.5 ± 6.1%), and CR (3.5 ± 1.5%) at expression levels, distribution, and number similar to those of the host interneurons (Fig. 6B–G). These results demonstrate that MGE-derived cells differentiate normally into mature interneurons under epileptogenic conditions and indicate that they are able to replace the loss of interneurons after SSP-Sap ablation. They also suggest that survival rate and normal maturation processes are not affected by this pathological condition.

Effects of the MGE-Derived Cell Grafts on the Inhibitory Activity

We wonder whether transplanted MGE precursors functionally integrate in the host brain, and if they are able to correct the alterations in the hippocampal inhibitory activity of the SSP-Sap-treated mice. We established three experimental groups: SSP-Sap ($n = 5$); SSP-Sap + MGE ($n = 5$); and sham-operated control ($n = 7$) (see Materials and Methods). The hippocampal area with interneuronal ablation containing GFP$^+$ cells was identified under epifluorescence, and IR-DIC visualized CA1 pyramidal neurons surrounded by GFP$^+$ cells were chosen for whole-cell patch-clamp recording. We compared the IPSC kinetic properties in CA1 pyramidal cells from each experimental group. BMI (10 μM) was also used at the end of the experiments to confirm that the IPSC were mediated by $GABA_A$ receptors (Fig 4A).

In accordance with the presence of GFP$^+$ GABAergic interneurons from the donor in the ablated area, we observed a significant increase in average sIPSC frequency and amplitude in CA1 pyramidal cells from SSP-Sap + MGE group, 2 months after transplantation (freq: 3.93 ± 0.47 Hz; $n = 17$; $p < 0.001$; amp: 18.60 ± 1.35 pA; $n = 17$; $p < 0.001$), when compared with the SSP-Sap group (values described above; $n = 17$) (Fig. 4A–D). There was a significant increase in the frequency and amplitude of sIPSC plotted as a cumulative distribution, consistent with an enhancement of GABAergic inhibition after the cell transplant (freq. and amp: K.S. test $p < 0.001$) (Fig. 4B, C). The amplitude distribution histogram showed a clear shift back to high-amplitude events in SSP-Sap + MGE group, similar to controls, which suggests an increase in the release of GABA from presynaptic sites in grafted animals (Fig. 4D).

Cumulative distribution and average mIPSc frequency in CA1 pyramidal cells from SSP-Sap + MGE group was also increased significantly (3.44 ± 0.25 Hz; $n = 17$; $p < 0.001$; Cumulative fraction K.S. test $p < 0.001$), reverting close to normality (Fig. 4E). Changes in mIPSC amplitude (SSP-Sap + MGE: 10.86 ± 0.37 pA; $n = 17$), and in average and histogram distribution of IPSC decay time constant or rise time 10–90%, were not observed (Fig. 4F, G; Fig. 5).

In order to verify the stability of the MGE graft effects on the hippocampal inhibitory input, we performed the same type of electrophysiological analysis at 4 months after the transplant. We obtained similar results in the study of IPSC kinetics, which strongly suggested a stable and maintained recuperation of GABAergic inhibitory levels along the time (Fig. 7).

MGE-Derived Cell Grafts Reduce Seizure Susceptibility

The observed imbalance in the GABAergic inhibition, due to the specific elimination of NK-1$^+$ interneurons, may have functional consequences on the normal behavior of the mice. To confirm this possibility, we monitored the animals for 2 months by video recording to detect spontaneous seizure. Additionally, we also evaluated their susceptibility to PTZ-induced seizures. As previously reported in the rat, no spontaneous behavioral seizures were observed in the SSP-Sap-injected mice. However, these mice presented a higher sensitivity to PTZ-induced seizures (Fig. 8). We compared the intensity and latency of seizures induced by PTZ (60 mg/kg, IP) in the SSP-Sap-treated mice ($n = 9$) and age-matched, sham-operated controls ($n = 9$). A greater number of animals from the SSP-Sap group developed severe seizures (56%: 5/9 reached stage V) when compared to control group (22%: 2/9) ($p < 0.0001$). While all the animals from the control group (9/9) exhibited mild seizures stages I–II, only 67% (6/9) of the SSP-Sap-treated mice developed seizures stages I–II ($p < 0.0001$) (Fig. 8A). Reciprocally, the percentage of severe seizures, stages IV–V, were higher in the SSP-Sap group (37%: 15/41, $n = 9$) when compared with the control group (13%: 8/63, $n = 9$; $p < 0.01$; (Fig. 8B). Finally, very interestingly, the mortality rate after PTZ-induced seizures was higher in the SSP-Sap group (56%) than in control group (22%) ($p < 0.0001$) (Fig. 8C).

The graft of MGE-derived cells recovered the

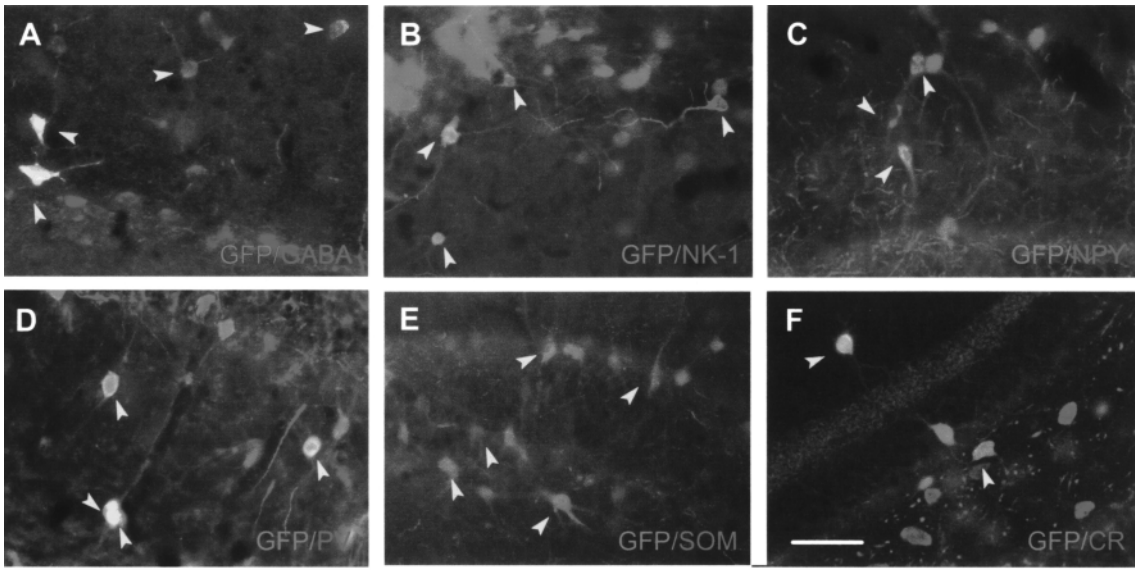

G. MGE graft-derived interneuron subtypes. (n=4)

Interneuron Marker	MGE Grafts in[1] SSP-Sap Model	MGE Grafts in[2] Normal Brain	MGE Grafts in[3] Kainate Model
GABA	64.6 ± 4.8%	42.8 ± 2.9%	68.8 ± 3.1%
PV	34.6 ± 5.6%	33.7 ± 4.7%	28.9 ± 3.1%
CR	3.5 ± 1.5%	10.3 ± 1.7%	30.8 ± 2.2%
NPY	18.8 ± 2.9%	13.1 ± 1.9%	7.8 ± 3.1

Figure 6. Molecular characterization of MGE graft-derived cells in the SSP-Sap-ablated hippocampus, 2 months after the transplant. Immunohistochemical colocalization of graft-derived GFP+ cells with typical mature interneuron markers, such as: GABA (A), NK-1 (B), NPY (C), PV (D), SOM (E), and CR (F). Arrowheads show double-positive cells. Scale bar: 25 μm. (G) Estimation of MGE graft-derived interneuron subtypes. Comparative of the generation of graft-derived GABAergic interneuron subpopulations under different conditions. [1]E12.5 mouse MGE cells transplanted in the SSP-Sap-ablated adult hippocampus. [2]E12.5 mouse MGE cells transplanted in the neonatal normal brain. Modified from Alvarez-Dolado et al. (2). [3]E15.5 rat MGE cells treated with FGF-2 and transplanted in the adult hippocampus of the kainite model of epilepsy. Modified from Hattiangady et al. (18).

GABA-mediated synaptic inhibition lost in SSP-Sap-treated animals (Figs. 4, 5, and 7). Therefore, transplantation of MGE precursors should have important consequences in the seizures susceptibility of these mice, as well. Significantly, the SSP-Sap + MGE group of mice presented lower percentage of severe seizure stage V (17%: 7/42, $n = 6$, $p < 0.05$) and low incidence of severe seizures (17%: 1/6) when compared with the SSP-Sap group ($p < 0.0001$) (Fig. 8A, B). In addition, they also exhibited a significant lower mortality rate (17%, $p < 0.0001$) than SSP-Sap-treated mice (Fig. 8C). The behavior of MGE-grafted mice in the PTZ assay was very similar to the sham-operated control group. No significant changes were found in the latency of seizures for all groups (control: 3.3 ± 0.8 s; SSP-Sap: 1.9 ± 0.6 s; SSP-Sap + MGE: 2.7 ± 0.8 s). Therefore, MGE-derived precursors were able to modulate the inhibitory circuitry in a pathological environment, increase the inhibitory synaptic input in CA1 hippocampal pyramidal cells, and, very importantly, decrease the level of seizure susceptibility.

DISCUSSION

In this work, we show that transplants of MGE-derived GABAergic precursors are able to replace, physically and functionally, the loss of hippocampal interneurons in a mouse model of seizure susceptibility. This is the first electrophysiological demonstration of an effect of the grafted cells on the altered circuitry of this murine seizure model. These cells restore the normal hippocampal synaptic activity and, what is more important, re-

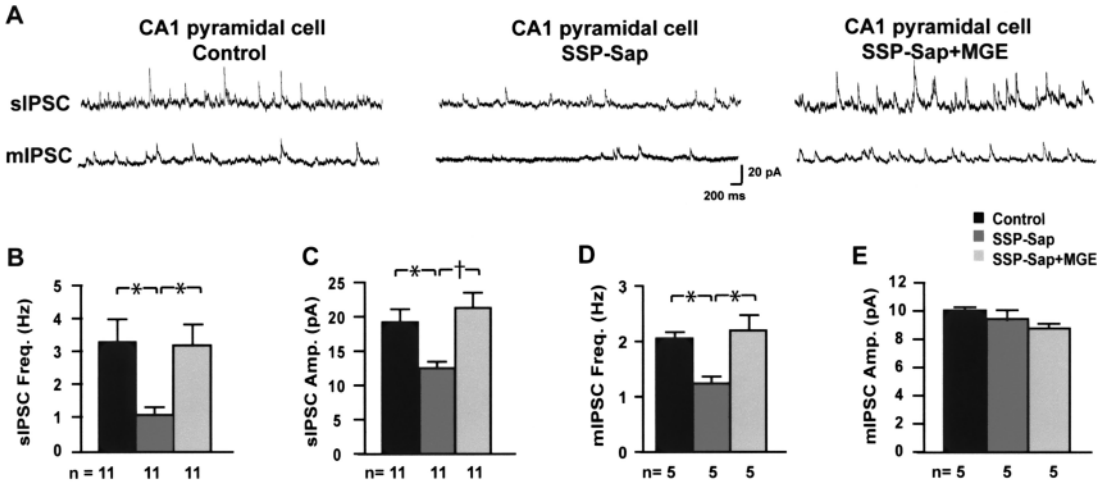

F - Kinetics of sIPSC and mIPSC in CA1 pyramidal cells

	Amplitude (pA)			Frequency (Hz)		
	Control	SSP-Sap	SSP-Sap+MGE	Control	SSP-Sap	SSP-Sap+MGE
sIPSC	19.22±1.89 (n=11)	12.51 ± 0.99[1, **] (n=11)	21.27 ± 2.24[2, §] (n=11)	3.43 ± 0.70 (n=11)	1.22 ± 0.21[1, **] (n=11)	3.23 ± 0.60[2, **] (n=11)
mIPSC	10.04±0.25 (n=5)	9.37 ± 0.70 (n=5)	8.74 ± 0.34 (n=5)	2.06 ± 0.11 (n=5)	1.25 ± 0.13[1, **] (n=5)	2.20 ± 1.42[2, **] (n=5)
	Decay time constant (ms)			**Rise time (10-90) (ms)**		
	Control	SSP-Sap	SSP-Sap+MGE	Control	SSP-Sap	SSP-Sap+MGE
sIPSC	7.78 ± 0.47 (n=10)	8.16 ± 0.32 (n=10)	7.51 ± 0.68 (n=10)	6.98 ± 0.42 (n=10)	7.01 ± 0.37 (n=10)	6.71 ± 0.11 (n=10)
mIPSC	6.80 ± 1.00 (n=5)	6.70 ± 0.50 (n=5)	7.03 ± 0.6 (n=5)	7.71 ± 0.70 (n=5)	7.53 ± 0.23 (n=5)	7.75 ± 0.56 (n=5)

Figure 7. MGE graft-derived cells are active 4 months after the transplant and rescue the normal synaptic inhibitory current in the hippocampus. (A) Amplitude and frequency of sIPSC and mIPSC in CA1 pyramidal cells from control, SSP-Sap-treated mice, and SSP-Sap + MGE groups 4 months after the transplant. Representative traces of sIPSC and mIPSC from CA1 pyramidal cells of the three experimental groups. (B–E) Plots of sIPSC and mIPSC from CA1 pyramidal cells of the three group of animals (black bar: control; dark gray bar: SSP-Sap; light gray bar: SSP-Sap + MGE). Note the decrease in sIPSC frequency and amplitude (B, C) and mIPSC frequency (D) on CA1 pyramidal cells from SSP-Sap mice when compared with controls (one-way ANOVA; $*p < 0.05$). In the SSP-Sap-treated mice grafted with MGE cells these values significantly increased when compared with SSP-Sap-treated animals with no MGE grafts (one-way ANOVA; $*p < 0.05$; $\dagger p < 0.01$). These increments reach levels similar to controls. (E) There was no difference in mIPCS amplitude on CA1 pyramidal cells between the three groups. Error bars indicate SEM; n = number of cells; sIPCS and mIPCS: spontaneous and miniature inhibitory postsynaptic currents, respectively. (F) Kinetics of sIPSC and mIPSC in CA1 pyramidal cells from age matched controls, and 4 months after SSP-Sap injection with no MGE grafts (SSP-Sap) and with MGE grafts (SSP-Sap + MGE). [1]Decreased IPSC amplitude and frequency in CA1 pyramidal cells of SSP-Sap mice. [2]Increased IPSC amplitude and frequency to control values in CA1 pyramidal cells of SSP-Sap mice 4 months after MGE grafts ($**p < 0.01$; $\S p < 0.01$, one-way ANOVA followed by Tukey-Kramer test). No changes in IPSC decay time constant or in rise time. Values are expressed in mean ± SEM. sIPSC: spontaneous IPSC; mIPCS: miniature IPSC; n = number of cells.

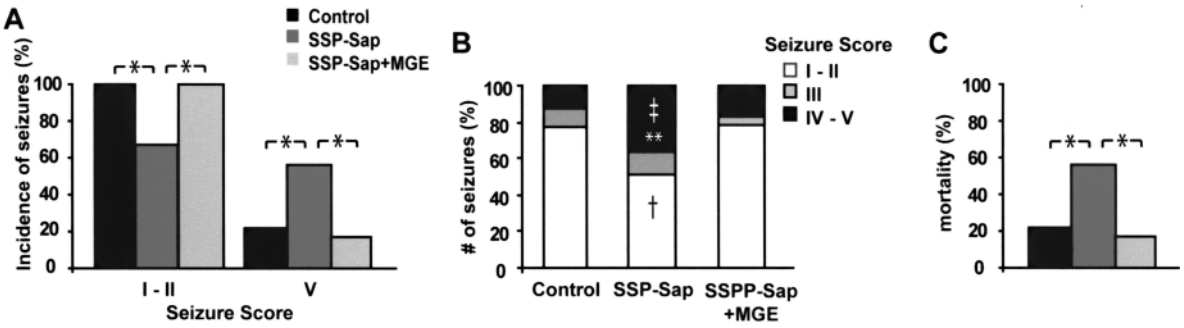

Figure 8. MGE-derived grafts reduce the susceptibility and mortality to PTZ induced seizures. (A) Plots of seizure incidence in mice treated with PTZ. The number of animals in the SSP-Sap group that exhibited seizure stage V (severe seizure) (5/9) was higher than in the control (2/9) and SSP-Sap + MGE (1/6) groups. Complementarily, the number of animals in SSP-Sap group that exhibited seizure stage I–II (6/9) was smaller than in control (9/9) and SSP-Sap + MGE groups (6/6). (B) Plots of PTZ-induced seizure rates. SSP-Sap-treated mice presented higher frequency of seizures stages IV–V (severe seizures) when compared with control (‡) and SSP-Sap + MGE mice (**). Complementarily, the frequency of seizure stages I–II (less intense seizures) was lower in the SSP-Sap group when compared with control and SSP-Sap + MGE mice (†). There was no difference in the intermediate seizure stage III for all groups. (C) Postseizure mortality of PTZ-treated mice. SSP-Sap-treated mice presented a higher mortality rate (56%) than control (22%) and SSP-Sap + MGE mice (17%). *$p < 0.0001$; ‡$p < 0.01$; **$p < 0.05$; †$p < 0.01$; Fisher's exact test.

duces the susceptibility and mortality to PTZ-induced seizures in the mice that received the transplant.

Creating a Disinhibited Environment

Defects in GABAergic system can lead to epilepsy. For this reason, to investigate the capacity of the MGE-derived precursor to repair these defects, we generated a mouse model characterized by the specific ablation of GABAergic interneurons in the hippocampus. There are other models of epilepsy (7,26,32,48). However, their mechanisms of seizure induction are multiple, and some of them present morphological changes that not always are observed in epileptic patients. For this reason, the precise elimination of interneurons with no gross morphological changes allows the study of specific alterations in the GABAergic system.

In this model, we eliminated the interneurons expressing NK-1 in the hippocampus by local injection of SSP-Sap as described earlier in rats (29). We did not observe significant differences comparing with rats. However, in mice the number of ablated PV^+ interneurons was smaller, due to the lack of NK-1 coexpression in most of the PV^+ interneurons (Fig. 2E–G). Nonetheless, the ablation of other GABAergic interneurons subpopulations ($NK\text{-}1^+$, SOM^+, or NPY^+) was sufficient to cause an important diminution in the synaptic inhibition and increment of excitability. This was evidenced by the decrease in IPSC on CA1 pyramidal cells and by increase in the susceptibility to PTZ-induced seizures, respectively. This is consistent with different animal models where small reduction in interneuron subpopulations leads to alterations in the inhibitory system and epilepsy (12,37).

Survival and Migration of MGE-Derived Grafted Cells

Similar to previous reports from our group and others (2,18,49), the MGE-derived cells that were transplanted in the adult brain survive for at least 1 year, with no signs of tumor formation. This indicates the stability and safety of the transplants.

In contrast, the survival rate of the transplanted cells in our hands (about 20%) was lower compared with other experimental models, such as kainate (18). There are multiple explanations for this difference. In the kainate model there is strong tissue damage, which may lead to neurotophin expression and therefore better survival. In contrast, our model lacks apparent histological damage. In addition, in the kainite model it was reported the transplant of cells from the whole ganglionic eminence of rats at later developmental stage (E15). These cells were pretreated with different factors (18), which may have improved their survival. Moreover, this seems to abolish their migratory capacity, provoking the formation of clusters that strongly alter the morphology of the brain parenchyma after the transplant. In our case (isolation of mouse MGE precursors at 12.5 embryonic day and no additional manipulation), two single cell injections per hemisphere were able to cover a wide area of the altered adult brain (Fig. 3), and no gross morphological alterations were observed. To our knowledge, these neuronal precursors are, up to now, the only ones with such migratory ability, which makes them ideal as delivery vectors.

Differentiation Into Mature Interneurons

MGE-derived cells expressed specific molecular markers of mature interneurons 2 months after the transplant.

Close to 70% of the total transplanted cells expressed GABA, the main inhibitory neurotransmitter in the CNS. This percentage probably is higher, since we observed an 86% of NeuN$^+$ cells, and no immunoreactivity for other neuronal subtypes like CaM kinase II, ChAT, and TH. These differences in the percentages may be due to an underestimation in GABA quantification causing low levels of expression and/or typical problems in the immunodetection of GABA. In addition, we also found oligodendrocytes (6%) and endothelial cells (8%), as previously reported (2).

The naturally occurring differentiation into GABAergic interneurons allowed the replacement of the SSP-Sap-ablated interneurons. It is interesting to note that, unlike other reports (21,27,45), the MGE-derived interneurons expressed GABA for long periods of time (1 year), without any further manipulation. In addition, the percentage of generation of each interneuronal subtype was not significantly affected by the ablated environment, compared with previous results of MGE grafts in normal mice (Fig. 6G) (2). We only observed a tendency of increment in the number and expression of NPY$^+$ cells. This is consistent with the reported overexpression of NPY in different animal models of epilepsy, such as pilocarpine (6,33).

However, we cannot discard that MGE-derived cells differentiate in a different way under other pathological conditions. In fact, comparing with a recent report, we observed a lower percentage of CR$^+$ cell differentiation in a model of kainate (Fig. 6G) (18). This could be due to differences in the origin of the cells (E15.5 rats vs. E12.5 mouse) and dissection procedures that may include part of the caudal ganglionic eminence. It may also due to the postmanipulation of the cells (they treat them with FGF-2) and their graft in a different pathological environment with higher damage levels, which may affect their survival rate, as indicated above. Further studies in several animal models of epilepsy should be performed to verify the appropriated differentiation of the MGE-derived cells in other epileptogenic environments.

Effects on the Local Synaptic Circuitry Activity

Previous works have shown partial improvements in epileptic symptoms after cell transplantation (22,27,42, 43,45). This was confirmed by the reduction in seizures incidence and the presence of graft-derived cells that expressed GABA. However, the morphological integration was poor and, importantly, electrophysiological records were not performed in the transplantation area. So, it cannot be concluded that the effects were due to the cell integration in the circuitry or by the secretion of GABA.

In a previous work (2), we demonstrated that MGE-derived cells acquire electrophysiological characteristics of fully mature interneurons after transplantation. In addition, these cells are able to perform synaptic contacts, confirmed by electron microscopy (49). Although here we did not present the intrinsic properties of the GFP$^+$ cells, our data provide electrophysiological evidence that MGE-derived cells are able to modify the inhibitory circuitry in a environment specifically altered by the ablation of GABAergic interneurons. The IPSC frequency and amplitude in the CA1 hippocampal pyramidal cells in SSP-Sap-treated mice reached values close to normal after MGE cell transplantation. To our knowledge, this is the first demonstration, at the electrophysiological level, that graft-derived cells are able to revert deficits in hippocampal synaptic inhibition. Moreover, given that MGE-derived cells do not differentiate into pyramidal neurons, it may be an excellent method for enhancement of inhibitory systems when and where needed, and in a long standing fashion.

Decrease in Seizure Susceptibility

PTZ assay is an effective method to screen AED (26). We used this assay to evaluate the effect of the MGE grafts on the seizures threshold of our mouse model. We found that transplantation reduced both the seizure susceptibility and, more importantly, the mortality due to PTZ-induced seizures. This was associated with widespread migration and differentiation of MGE-derived cells into functionally mature interneurons, and in line with the observed increment in the inhibitory synaptic activity in the CA1 of the hippocampus. These results demonstrate that MGE-derived grafts have effects on the behavior of the host animal and show their capacity to decrease seizure susceptibility.

CONCLUSION

Our results strongly support the use of MGE-derived cells to repair defects in the GABAergic system and increase the inhibitory input. They fulfill most of the requirements for an appropriate cell-based therapy: a satisfactory stability, survival, and safety; their extensive migration; the differentiation into functionally mature interneurons (which imply the integration into the local circuitry and modulation of its activity); and, very importantly, the ability to rescue the GABAergic defects and revert the symptomatology in the animal model of seizure susceptibility.

Our results evidence the suitability of MGE-derived cells for the treatment of epilepsies associated with GABAergic alterations, absence of interneurons, or with deficits in inhibition. However, the etiology of epilepsy is multiple and it is not clear whether this cell type may improve the condition in all cases. We should be cautious before use in the clinic. Further efforts should be devoted to demonstrate the mechanism of action of MGE-derived cells, and to verify their efficacy in other

models of epilepsy in which alterations of the GABAergic system are not the main cause.

ACKNOWLEDGMENTS: We thank Mercedes Paredes for reviewing the manuscript. This work was supported by grants from Spanish Ministry of Science and Innovation (SAF 07/61880 and FIS 07/0079), and the Regenerative Medicine Programme from CIPF. M.E.C. and I.Z. were recipients of Miguel Servet contract from Carlos III Institute (Spanish Ministry of Science and Innovation) and Ph.D. fellowship from Generalitat Valenciana, respectively.

REFERENCES

1. Acsady, L.; Katona, I.; Gulyas, A. I.; Shigemoto, R.; Freund, T. F. Immunostaining for substance P receptor labels GABAergic cells with distinct termination patterns in the hippocampus. J. Comp. Neurol. 378(3):320–336; 1997.
2. Alvarez-Dolado, M.; Calcagnotto, M. E.; Karkar, K. M.; Southwell, D. G.; Jones-Davis, D. M.; Estrada, R. C.; Rubenstein, J. L.; Alvarez-Buylla, A.; Baraban, S. C. Cortical inhibition modified by embryonic neural precursors grafted into the postnatal brain. J. Neurosci. 26(28): 7380–7389; 2006.
3. Anderson, S. A.; Kaznowski, C. E.; Horn, C.; Rubenstein, J. L.; McConnell, S. K. Distinct origins of neocortical projection neurons and interneurons in vivo. Cereb. Cortex 12(7):702–709; 2002.
4. Arellano, J. I.; Munoz, A.; Ballesteros-Yanez, I.; Sola, R. G.; DeFelipe, J. Histopathology and reorganization of chandelier cells in the human epileptic sclerotic hippocampus. Brain 127(Pt. 1):45–64; 2004.
5. Austin, J. E.; Buckmaster, P. S. Recurrent excitation of granule cells with basal dendrites and low interneuron density and inhibitory postsynaptic current frequency in the dentate gyrus of macaque monkeys. J. Comp. Neurol. 476(3):205–218; 2004.
6. Baraban, S. C.; Tallent, M. K. Interneuron Diversity series: Interneuronal neuropeptides—endogenous regulators of neuronal excitability. Trends Neurosci. 27(3):135–142; 2004.
7. Ben-Ari, Y.; Cossart, R. Kainate, a double agent that generates seizures: Two decades of progress. Trends Neurosci. 23(11):580–587; 2000.
8. Bulic-Jakus, F.; Ulamec, M.; Vlahovic, M.; Sincic, N.; Katusic, A.; Juric-Lekc, G.; Serman, L.; Kruslin, B.; Belicza, M. Of mice and men: Teratomas and teratocarcinomas. Coll. Antropol. 30(4):921–924; 2006.
9. Butt, S. J.; Fuccillo, M.; Nery, S.; Noctor, S.; Kriegstein, A.; Corbin, J. G.; Fishell, G. The temporal and spatial origins of cortical interneurons predict their physiological subtype. Neuron 48(4):591–604; 2005.
10. Buzsaki, G.; Ponomareff, G.; Bayardo, F.; Shaw, T.; Gage, F. H. Suppression and induction of epileptic activity by neuronal grafts. Proc. Natl. Acad. Sci. USA 85(23): 9327–9330; 1988.
11. Calcagnotto, M. E.; Paredes, M. F.; Tihan, T.; Barbaro, N. M.; Baraban, S. C. Dysfunction of synaptic inhibition in epilepsy associated with focal cortical dysplasia. J. Neurosci. 25(42):9649–9657; 2005.
12. Cobos, I.; Calcagnotto, M. E.; Vilaythong, A. J.; Thwin, M. T.; Noebels, J. L.; Baraban, S. C.; Rubenstein, J. L. Mice lacking Dlx1 show subtype-specific loss of interneurons, reduced inhibition and epilepsy. Nat. Neurosci. 8(8):1059–1068; 2005.
13. Daadi, M. M.; Lee, S. H.; Arac, A.; Grueter, B. A.; Bhatnagar, R.; Maag, A. L.; Schaar, B.; Malenka, R. C.; Palmer, T. D.; Steinberg, G. K. Functional engraftment of the medial ganglionic eminence cells in experimental stroke model. Cell Transplant. 18(7):815–826; 2009.
14. Duncan, J. S. The outcome of epilepsy surgery. J. Neurol. Neurosurg. Psychiatry 70(4):432; 2001.
15. During, M. J.; Ryder, K. M.; Spencer, D. D. Hippocampal GABA transporter function in temporal-lobe epilepsy. Nature 376(6536):174–177; 1995.
16. Eaton, M. J.; Plunkett, J. A.; Martinez, M. A.; Lopez, T.; Karmally, S.; Cejas, P.; Whittemore, S. R. Transplants of neuronal cells bioengineered to synthesize GABA alleviate chronic neuropathic pain. Cell Transplant. 8(1):87–101; 1999.
17. Hadjantonakis, A. K.; Gertsenstein, M.; Ikawa, M.; Okabe, M.; Nagy, A. Generating green fluorescent mice by germline transmission of green fluorescent ES cells. Mech. Dev. 76(1–2):79–90; 1998.
18. Hattiangady, B.; Rao, M. S.; Shetty, A. K. Grafting of striatal precursor cells into hippocampus shortly after status epilepticus restrains chronic temporal lobe epilepsy. Exp. Neurol. 212(2):468–481; 2008.
19. Jacobs, M. P.; Fischbach, G. D.; Davis, M. R.; Dichter, M. A.; Dingledine, R.; Lowenstein, D. H.; Morrell, M. J.; Noebels, J. L.; Rogawski, M. A.; Spencer, S. S.; Theodore, W. H. Future directions for epilepsy research. Neurology 57(9):1536–1542; 2001.
20. Kobayashi, M.; Buckmaster, P. S. Reduced inhibition of dentate granule cells in a model of temporal lobe epilepsy. J. Neurosci. 23(6):2440–2452; 2003.
21. Kokaia, M.; Aebischer, P.; Elmer, E.; Bengzon, J.; Kalen, P.; Kokaia, Z.; Lindvall, O. Seizure suppression in kindling epilepsy by intracerebral implants of GABA- but not by noradrenaline-releasing polymer matrices. Exp. Brain Res. 100(3):385–394; 1994.
22. Kriegstein, A. R.; Pitkanen, A. Commentary: The prospect of cell-based therapy for epilepsy. Neurotherapeutics 6(2): 295–299; 2009.
23. Kwan, P.; Brodie, M. J. Early identification of refractory epilepsy. N. Engl. J. Med. 342(5):314–319; 2000.
24. Lindvall, O.; Barry, D. I.; Kikvadze, I.; Brundin, P.; Bolwig, T. G.; Bjorklund, A. Intracerebral grafting of fetal noradrenergic locus coeruleus neurons: Evidence for seizure suppression in the kindling model of epilepsy. Prog. Brain Res. 78:79–86; 1988.
25. Lloyd, K. G.; Bossi, L.; Morselli, P. L.; Munari, C.; Rougier, M.; Loiseau, H. Alterations of GABA-mediated synaptic transmission in human epilepsy. Adv. Neurol. 44: 1033–1044; 1986.
26. Loscher, W. Animal models of epilepsy for the development of antiepileptogenic and disease-modifying drugs. A comparison of the pharmacology of kindling and post-status epilepticus models of temporal lobe epilepsy. Epilepsy Res. 50(1–2):105–123; 2002.
27. Loscher, W.; Ebert, U.; Lehmann, H.; Rosenthal, C.; Nikkhah, G. Seizure suppression in kindling epilepsy by grafts of fetal GABAergic neurons in rat substantia nigra. J. Neurosci. Res. 51(2):196–209; 1998.
28. Marin, O.; Rubenstein, J. L. A long, remarkable journey: Tangential migration in the telencephalon. Nat. Rev. Neurosci. 2(11):780–790; 2001.
29. Martin, J. L.; Sloviter, R. S. Focal inhibitory interneuron loss and principal cell hyperexcitability in the rat hippocampus after microinjection of a neurotoxic conjugate of saporin and a peptidase-resistant analog of Substance P. J. Comp. Neurol. 436(2):127–152; 2001.

30. Medina, A. E.; Manhaes, A. C.; Schmidt, S. L. Sex differences in sensitivity to seizures elicited by pentylenetetrazol in mice. Pharmacol. Biochem. Behav. 68(3):591–596; 2001.
31. Meldrum, B. S. Epilepsy and gamma-aminobutyric acid-mediated inhibition. Int. Rev. Neurobiol. 17:1–36; 1975.
32. Mello, L. E.; Cavalheiro, E. A.; Tan, A. M.; Kupfer, W. R.; Pretorius, J. K.; Babb, T. L.; Finch, D. M. Circuit mechanisms of seizures in the pilocarpine model of chronic epilepsy: Cell loss and mossy fiber sprouting. Epilepsia 34(6):985–995; 1993.
33. Morimoto, K.; Fahnestock, M.; Racine, R. J. Kindling and status epilepticus models of epilepsy: rewiring the brain. Prog. Neurobiol. 73(1):1–60; 2004.
34. Nakaya, Y.; Kaneko, T.; Shigemoto, R.; Nakanishi, S.; Mizuno, N. Immunohistochemical localization of substance P receptor in the central nervous system of the adult rat. J. Comp. Neurol. 347(2):249–274; 1994.
35. Nilsen, K. E.; Cock, H. R. Focal treatment for refractory epilepsy: hope for the future? Brain Res. Brain Res. Rev. 44(2–3):141–153; 2004.
36. Paxinos, G.; Franklin, K. B. J. The mouse brain in stereotaxic coordinates, compact 2nd ed. Amsterdam, Netherlands: Elsevier Academic Press; 2004.
37. Powell, E. M.; Campbell, D. B.; Stanwood, G. D.; Davis, C.; Noebels, J. L.; Levitt, P. Genetic disruption of cortical interneuron development causes region- and GABA cell type-specific deficits, epilepsy, and behavioral dysfunction. J. Neurosci. 23(2):622–631; 2003.
38. Raedt, R.; Van Dycke, A.; Vonck, K.; Boon, P. Cell therapy in models for temporal lobe epilepsy. Seizure 16(7): 565–578; 2007.
39. Ribak, C. E.; Harris, A. B.; Vaughn, J. E.; Roberts, E. Inhibitory, GABAergic nerve terminals decrease at sites of focal epilepsy. Science 205(4402):211–214; 1979.
40. Richardson, R. M.; Barbaro, N. M.; Alvarez-Buylla, A.; Baraban, S. C. Developing cell transplantation for temporal lobe epilepsy. Neurosurg. Focus 24(3–4):E17; 2008.
41. Ruschenschmidt, C.; Koch, P. G.; Brustle, O.; Beck, H. Functional properties of ES cell-derived neurons engrafted into the hippocampus of adult normal and chronically epileptic rats. Epilepsia 46(Suppl. 5):174–183; 2005.
42. Shetty, A. K.; Turner, D. A. Fetal hippocampal grafts containing CA3 cells restore host hippocampal glutamate decarboxylase-positive interneuron numbers in a rat model of temporal lobe epilepsy. J. Neurosci. 20(23):8788–8801; 2000.
43. Shetty, A. K.; Zaman, V.; Hattiangady, B. Repair of the injured adult hippocampus through graft-mediated modulation of the plasticity of the dentate gyrus in a rat model of temporal lobe epilepsy. J. Neurosci. 25(37):8391–8401; 2005.
44. Sloviter, R. S.; Ali-Akbarian, L.; Horvath, K. D.; Menkens, K. A. Substance P receptor expression by inhibitory interneurons of the rat hippocampus: enhanced detection using improved immunocytochemical methods for the preservation and colocalization of GABA and other neuronal markers. J. Comp. Neurol. 430(3):283–305; 2001.
45. Thompson, K. Transplantation of GABA-producing cells for seizure control in models of temporal lobe epilepsy. Neurotherapeutics 6(2):284–294; 2009.
46. Thompson, K. W. Genetically engineered cells with regulatable GABA production can affect afterdischarges and behavioral seizures after transplantation into the dentate gyrus. Neuroscience 133(4):1029–1037; 2005.
47. Thompson, K. W.; Suchomelova, L. M. Transplants of cells engineered to produce GABA suppress spontaneous seizures. Epilepsia 45(1):4–12; 2004.
48. Turski, W. A.; Cavalheiro, E. A.; Schwarz, M.; Czuczwar, S. J.; Kleinrok, Z.; Turski, L. Limbic seizures produced by pilocarpine in rats: Behavioural, electroencephalographic and neuropathological study. Behav. Brain Res. 9(3):315–335; 1983.
49. Wichterle, H.; Garcia-Verdugo, J. M.; Herrera, D. G.; Alvarez-Buylla, A. Young neurons from medial ganglionic eminence disperse in adult and embryonic brain. Nat. Neurosci. 2(5):461–466; 1999.
50. Wierenga, C. J.; Wadman, W. J. Miniature inhibitory postsynaptic currents in CA1 pyramidal neurons after kindling epileptogenesis. J. Neurophysiol. 82(3):1352–1362; 1999.
51. Wonders, C.; Anderson, S. A. Cortical interneurons and their origins. Neuroscientist 11(3):199–205; 2005.
52. Zaman, V.; Shetty, A. K. Fetal hippocampal CA3 cell grafts enriched with fibroblast growth factor-2 exhibit enhanced neuronal integration into the lesioned aging rat hippocampus in a kainate model of temporal lobe epilepsy. Hippocampus 13(5):618–632; 2003.
53. Zappone, C. A.; Sloviter, R. S. Translamellar disinhibition in the rat hippocampal dentate gyrus after seizure-induced degeneration of vulnerable hilar neurons. J. Neurosci. 24(4):853–864; 2004.